VALIZADEH, S., LAWAL, S.M., FOUGH, N. and SHOKRI, A. 2024. Analyzing efficiency and temperature variations in PSC structures utilizing $RbGeBr_3$. In: *Proceedings of the 6th Global power, energy and communication conference 2024 (GPECOM2024), 4-6 June 2024, Budapest, Hungary*. Piscataway: IEEE [online], pages 334-338. Available from: https://doi.org/10.1109/GPECOM61896.2024.10582665

# Analyzing efficiency and temperature variations in PSC structures utilizing $RbGeBr_3$.

VALIZADEH, S., LAWAL, S.M., FOUGH, N. and SHOKRI, A.

2024

# Analyzing Efficiency and Temperature Variations in PSC Structures Utilizing $RbGeBr_3$


Shima Valizadeh
Department of Theoretical Physics and Nano
Alzahra University,
Tehran, Iran
sh.valizadeh59@gmail.com

Sani Mohammed Lawal
School of Engineering
Robert Gordon University
United Kingdom
s.lawal1@rgu.ac.uk

Nazila Fough
School of Engineering
Robert Gordon University
United Kingdom
n.fough1@rgu.ac.uk

Aliasghar Shokri
Department of Theoretical Physics and Nano
Alzahra University,
Tehran, Iran
aashokri@alzahra.ac.ir



***Abstract*— This paper investigates the utilization of $eB_3$ as an absorbing layer in two types of perovskite solar cells. The investigation involves systematic adjustments in the thicknesses of both the $eB_3$ as absorber layer and the electron transfer layer. The Poisson, continuity, and transport equations are solved using the finite element method. Gold was chosen as the electrode's metal contact. Furthermore, the study investigates the effect of temperature fluctuations on the efficiency of these systems. The FTO/ITO/ $eB_3$ /PEDOT: PSS/Au configuration has the highest power conversion efficiency (11.37%), with a short-circuit current of 14.472 mA/cm² and an open-circuit voltage of 0.96 V. Furthermore, an alternative structure, FTO/TiO2/ $eB_3$ /CuSCN/Au, is investigated, resulting in power conversion efficiencies of 10.58%. These findings have important implications for the development of more advanced and efficient perovskite solar cells with mineral perovskite layers.**



***Keywords*— Perovskite solar cell, photovoltaic, Inorganic absorber layer, efficiency, COMSOL Multiphysics simulator.**


## I. Introduction

In the last few decades, one of the issues that the scientific community has been dealing with is finding scientific, safe, and affordable solutions to prevent global warming. Perhaps the most likely solution to this issue is to harness the pure energies that nature provides [1]. Utilizing the sun's copious thermal and light energy is a practical approach. [1]. This freely accessible renewable resource has enormous potential because it produces an incredible amount of $1.5 \times 10^{18}$ kWh/year of radiation annually, which is roughly 100 times the energy produced by all fossil fuels combined. As a result, researchers created photovoltaic technology, which made it possible to use solar energy, which has own distinct advantages and limitations [2-4]. One of the newly developed solar cells, Perovskite Solar Cells(PSCs), had shown a notable increase in efficiency over the past decade, going from 3.8% to 25.5% [3,5]. Organic-inorganic perovskite materials are most frequently utilized as the light-absorbing layer in these solar cells. PSCs still have issues with humidity and temperature sensitivity, though [6, 7]. For the purpose of creating all-inorganic PSCs with improved optoelectronic performance and stability, researchers have investigated the use of inorganic cations like K, Rb, and Cs in perovskite unit cells [8,9]. It was found that by switching from organic-mineral perovskite material to inorganic perovskite material, the solar cell's stability time against environmental variables like humidity and temperature increased [10,11,12].

Perovskite materials come in a wide range, which has led to considerable research into their potential applications in solar cells and other electrical devices. The objective of this study is to examine how mineral perovskite, $RbGeBr_3$, behaves as a light-absorbing layer in two configurations, with distinct layers for the transport of holes and electrons and gold as an electrode for electron collection. Additionally, the COMSOL Multiphysics Simulator is also utilised for educational purposes. Four pivotal factors are carefully compared and assessed across distinct architectures: the short-circuit current ($J_{sc}$), the open circuit voltage ($V_{oc}$), the Fill Factor (FF), and the Power Conversion Efficiency (PCE).

## II. Structure Design of Desired PSCs

Perovskite materials are widely available in nature and have several advantageous qualities, including balanced electron-hole transport, a direct band gap, low exciton binding energy, minimal crystal defects, high charge mobility, low production costs, and high efficiency. These materials are utilized in these cells [13, 14]. Notably, neither theoretically nor empirically has the function of $RbGeBr_3$ as an inorganic material in a solar cell been studied; this work attempts to close this knowledge gap [15]. Therefore, the main goal of this study was to investigate the light-absorbing properties of the mineral $RbGeBr_3$ in two various PSC architectures. Fig 1 depicts the crystal structure of cubic halide perovskite $RbGeBr_3$, which has a direct bandgap of 1.49 eV [16,17].

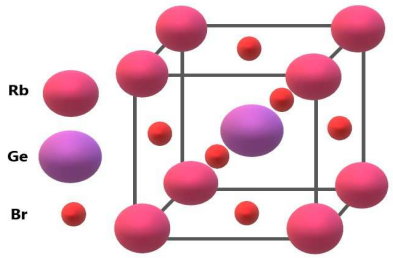


Fig 1, Crystal structure of cubic halide perovskites $ABX_3$ (A =, Rb; X = Br. Redrawn with modification from [16, 17].

Fig 2 illustrates the general operating principle of PSCs, which presents an overview of the electrostatic structure of a PSCs. The initial configuration of PSCs consisted of the organic material PEDOT:PSS in the HTL and the semiconductor material ITO in the ETL [18,19, 20]. The semiconductor materials for the ETL and HTL in the second structure are TiO2 and CuSCN, respectively, and are accompanied by an Au metal electrode [21–25].

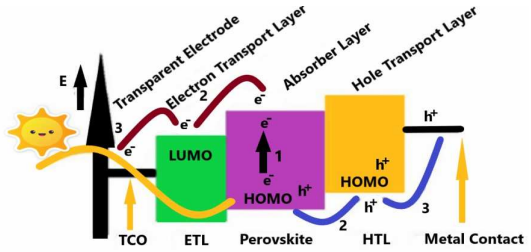


Fig 2, The electrostatic structure of a PSCs overall performance.

The following is the desired multilayer sequence for this study, depicted by the first and second desired configurations:

A. FTO/ ITO/ $RbGeBr_3$/ PEDOT:PSS/ Au
B. FTO/ $TiO_2$/ $RbGeBr_3$/ CuSCN/ Au

## III. Simulation Details

In this study, the COMSOL simulator employs the semiconductor module in a two-dimensional context [26]. Additionally, optical properties play a crucial role, especially the refractive index and its intrinsic features, which are given in equation below. Equation1[16]:

$$N(\omega) = n(\omega) + ik(\omega) \quad (1)$$

n(ω), which denotes the material's light reflection, and the imaginary part k(ω), which is crucial to the solar cell simulation and in responsibility of the material's absorption of the sun's spectrum. Understanding the chosen material's absorption coefficient—one of its inherent properties—is another crucial component of a solar cell. The absorption coefficient of the desired material has a direct relationship with the photoelectron generation rate in a solar cell. The absorption coefficient is defined by the equation $\alpha(\lambda) = \frac{4\pi k(\lambda)}{\lambda}$ [16]. This absorption coefficient is essential for determining how the material affects incident light, particularly in the solar spectrum at 1.5 AM. The following equation is shown how to calculate the generation rate of carriers [16]:

$$G(x,\lambda) = \frac{4\pi}{hc}\int_{\lambda_1}^{\lambda_2} k(\lambda)\Phi(\lambda)exp(-\alpha(\lambda)x)d\lambda \quad (2)$$

Here $\Phi(\lambda)$ illustrates the solar spectrum. The incident wavelength range is specified with $\lambda_1$ at 300 nm and $\lambda_2$ at 800 nm. In Fig 3 presents the absorption coefficient $RbGeBr_3$ substance [17].

Furthermore, the equations depicted below can be utilized to determine the cell's [27]:

$$I = I_{ph} - I_D = I_{ph} - I_0[\exp\left[\frac{eV}{K_B T_c}\right] - 1] \quad (3)$$

The net current I is calculated by difference between the photon current, $I_{ph}$, and the ideal current of the diode, $I_D$. $I_0$ shows the dark saturation current, which is highly dependent on temperature. Equation 4 presents the open-circuit voltage [27]:

$$V_{oc} = \left(\frac{K_B T}{q}\right)\ln\left(\frac{J_{sc}}{J_0}\right) \quad (4)$$

The final efficiency is shown in equation [28]:

$$\eta = \frac{P_{max}}{P_{in}} = \frac{I_{max}V_{max}}{P_{in}} \quad (5)$$

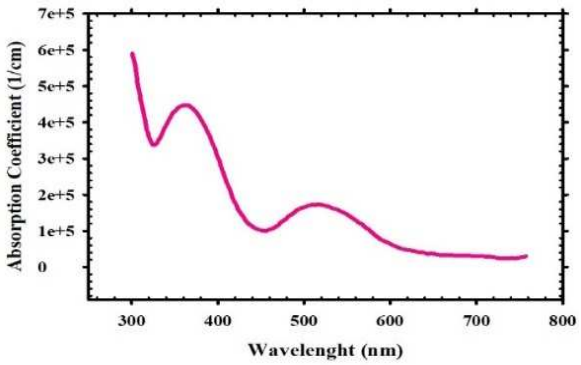


Fig 3, the absorption coefficient Rb material. Redraw [17]

In this case, the light input power is represented as $P_{in}$, which is equivalent to 100 mW/cm$^2$. Furthermore, it is also significant to understand that temperature variations cause semiconductor materials to alter in terms of their electrical properties. Hence, the PSCs' electrical properties exhibit changes in response to temperature. Notably, temperature affects predominantly on the open circuit voltage of the solar cell, while the impact on the short circuit current density remains minimal. The effects of temperature on voltage are described by the following equations [29]:

$$\frac{dV_{oc}}{dT} = -\frac{(V_{g0}-V_{oc})+3V_T}{T} + V_T\left(\frac{1}{J_{sc}}\frac{d}{d_T}J_{sc} + \frac{1}{V_T}\frac{d}{dT}V_g\right) \quad (6)$$

Two parameters are clearly defined: the thermal voltage defined as $V_t = \frac{KT}{q}$, where K is the Boltzman constant, T is the temperature, and q is the elementary charge and the energy gap voltage denoted as $V_g = \frac{E_g}{q}$, where $E_g$ is the energy gap.

## IV. Discussions and Results

The main purpose of this study is to choose the most efficient and optimal configuration among the two given structural desired in section 2, in order to obtain the maximum efficiency. To find out which of these two structures was the most efficient, two cases were looked at first. First, increase the thickness of the light absorber layer from 200 nm to 500 nm while keeping the electron transport layer at a constant 80 nm. Secondly, keep the light-absorbing layer at a constant 200 nm thickness while increasing the thickness of the electron transport layer from 80 nm to 110 nm. Moreover, to compare the performance and PCE of the best configuration, the four vital parameters of the solar cell, namely $J_{sc}$, $V_{oc}$, FF, and PCE, have also been computed. For

every structure, graphs illustrating the final results of these computations are given. Furthermore, the PCE of these architectures is being evaluated in relation to increases in temperature while operating at their respective maximum efficiency levels. Moreover, the current density – voltage(J-V) and output power- voltage(P-V) are plotted for all distinct structures.

### *A. FTO/ ITO/ $RbGeBr_3$/ PEDOT: PSS / Au*

In this scenario, Fig 4a shows the solar cell's short circuit, resulting in the maximum level of generated current and the open circuit voltage is approximately 0.96 V, representing the highest voltage. The highest power is shown in Fig 4b.

a. T=300K

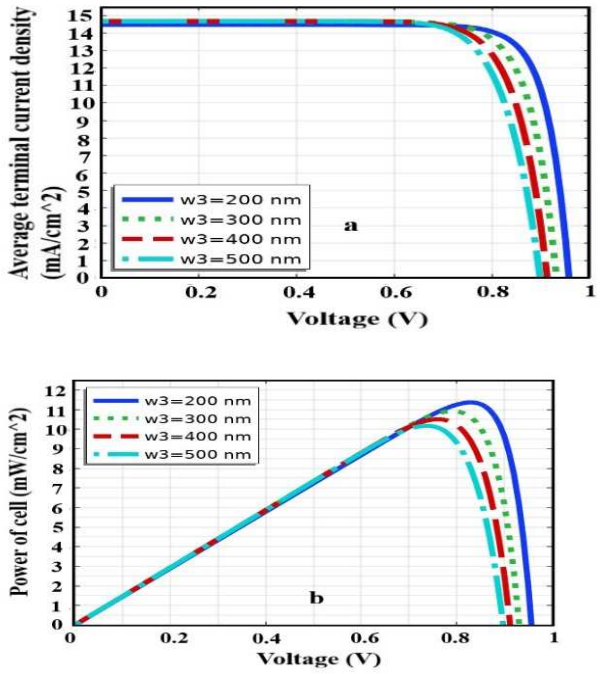


Fig 4, a) the current-voltage (J-V), b) Power of cell (P-V) at 300 K

Tables 1 and 2 illustrate all the four factors, which have been computed in both scenarios, that were mentioned above:

TABLE 1 FOUR FACTORS OF SOLAR CELLS CALCULATION FOR THE FIRST SCENARIO

| **The First Scenario** | | | | | |
|---|---|---|---|---|---|
| *The First Structure* | | *FTO/ITO/$RbGeBr_3$/PEDOT:PSS/Au* | | | |
| The Four Factors | | Jsc (mA/cm²) | Voc (V) | Fill Factor | PCE% |
| *Thicknesses (nm)* | | | | | |
| *Light-absorbing layer=200* | *ETL =80* | 14.472 | 0.96 | 0.81 | 11.37 |
| *Light-absorbing layer=300* | *ETL =80* | 14.66 | 0.93 | 0.80 | 10.92 |
| *Light-absorbing layer=400* | *ETL =80* | 14.67 | 0.91 | 0.78 | 10.50 |
| *Light-absorbing layer=500* | *ETL =80* | 14.67 | 0.89 | 0.77 | 10.17 |

TABLE 2 FOUR FACTORS OF SOLAR CELLS CALCULATION FOR THE SECOND SCENARIO

| **The Second Scenario** | | | | | |
|---|---|---|---|---|---|
| *The First Structure* | | *FTO/ ITO /$RbGeBr_3$/ PEDOT:PSS /Au* | | | |
| The Four Factors | | Jsc (mA/cm) | Voc (V) | Fill Factor | PCE% |
| *Thicknesses (nm)* | | | | | |
| *Light-absorbing layer=200* | *ETL =80* | 14.472 | 0.96 | 0.81 | 11.37 |
| *Light-absorbing layer=200* | *ETL =90* | 11.68 | 0.96 | 0.81 | 9.16 |
| *Light-absorbing layer=200* | *ETL =100* | 9.43 | 0.95 | 0.82 | 7.37 |
| *Light-absorbing layer=200* | *ETL =110* | 7.61 | 0.95 | 0.82 | 5.94 |

b. T= 450K

In the next step, the temperature varied from 300 K to 450 K. This effect of increasing temperature was investigated on the first structure, FTO/ ITO / $RbGeBr_3$/ PEDOT: PSS / Au, at the highest final efficiency. Temperature altering has a minimal impact on the short circuit current in this structure (Fig 5a). Nevertheless, the open circuit voltage dropped by 0.3 volts for the first structure, which is directly proportional to temperature based on equation 6 (Fig 5b).

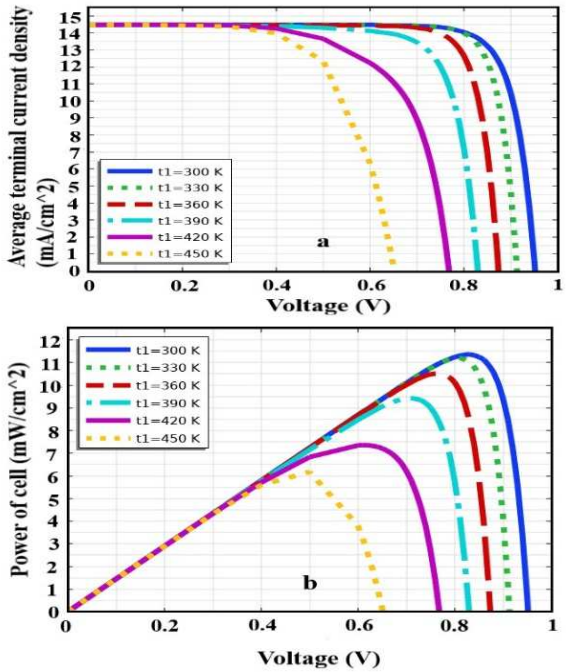


Fig 5, Variation of solar cell parameters with the Operating temperature .5a) The short circuit current density (mA/cm²), 5b) The open circuit voltage (V), with variation of temprature from 300K to 450K.

### *B. FTO/ $TiO_2$/$RbGeBr_3$/CuSCN/Au*

a. T=300K

In the second structure, similar to the first structure mentioned previously, the impact of two scenarios is investigated on the configuration:

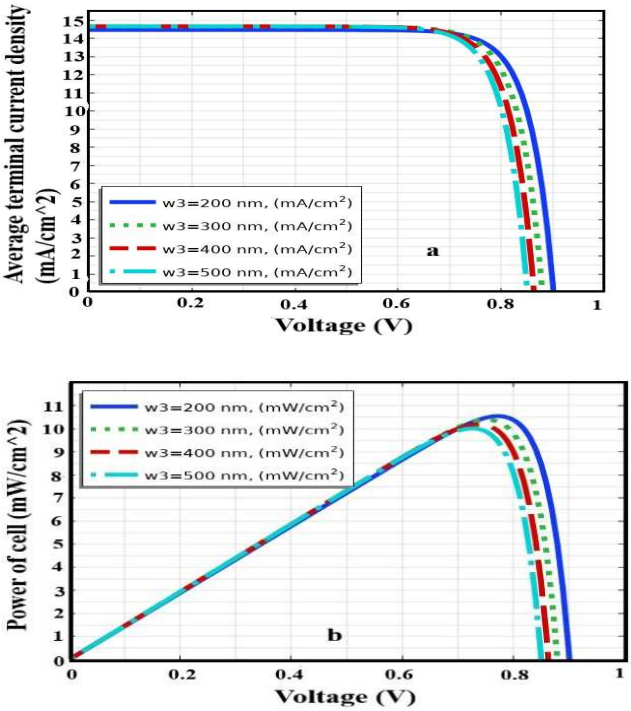


Fig 6.a) shows the current-voltage (J-V), b) Power of cell (P-V) at 300 K

The highest short circuit current is approximately 14.467 mA/cm², also the open circuit voltage is obtained 0.9 V (Fig 6a). The maximum power is generated by the solar cell as presented in Fig 6b. Additionally, Table 3 and 4 denote the influence of the absorber layer and the ETL thickness on the important factors of the solar cell, respectively.

TABLE 3 FOUR FACTORS OF SOLAR CELLS CALCULATION FOR THE FIRST SCENARIO

| **The First Scenario** | | | | | |
|---|---|---|---|---|---|
| *The Second Structure* | | *FTO/TiO2/RbGeBr$_3$/CuSCN/Au* | | | |
| The Four Factors | | Jsc (mA/cm²) | Voc (V) | Fill Factor | PCE% |
| *Thicknesses (nm)* | | | | | |
| *Light-absorbing layer=200* | *ETL =80* | 14.467 | 0.9 | 0.81 | 10.58 |
| *Light-absorbing layer=300* | *ETL =80* | 14.671 | 0.88 | 0.80 | 10.41 |
| *Light-absorbing layer=400* | *ETL =80* | 14.682 | 0.87 | 0.79 | 10.20 |
| *Light-absorbing layer=500* | *ETL =80* | 14.684 | 0.86 | 0.79 | 10.00 |

a. T=450K

Same architecture, FTO/TiO2/ $RbGeBr_3$ /CuSCN/Au, when it has obtained the highest PCE, the impact of temperature increasing is investigated on it. In conclusion, this structure's highest efficiency is determined at 200 nm for the absorber layer, 80 nm for the ETL, and 300 K for the temperature. The results are given in Table 5.

TABLE 4 FOUR FACTORS OF SOLAR CELLS CALCULATION FOR THE SECOND SCENARIO

| **The Second Scenario** | | | | | |
|---|---|---|---|---|---|
| *The Second Structure* | | *FTO/TiO2RbGeBr$_3$/CuSCN/Au* | | | |
| The Four Factors | | Jsc (mA/cm²) | Voc (V) | Fill Factor | PCE% |
| *Thicknesses (nm)* | | | | | |
| *Light-absorbing layer=200* | *ETL= 80* | 14.467 | 0.9 | 0.81 | 10.58 |
| *Light-absorbing layer=200* | *ETL= 90* | 11.686 | 0.89 | 0.80 | 8.42 |
| *Light-absorbing layer=200* | *ETL= 100* | 9.434 | 0.89 | 0.80 | 6.73 |
| *Light-absorbing layer=200* | *ETL= 110* | 7.617 | 0.88 | 0.79 | 5.35 |

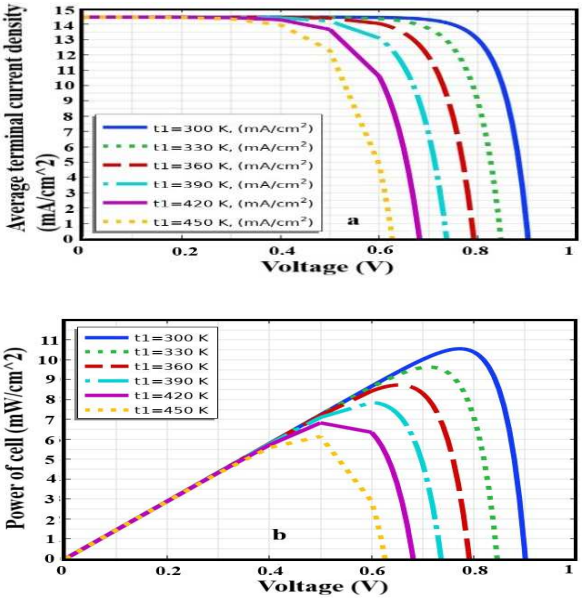


Fig 7, Variation of solar cell parameters with the Operating temperature .7a) The short circuit current density (mA/cm²), 7b) The open circuit voltage (V), with variation of temprature from 300K to 450K.

Table 5 denots the PCE% related to the two proposed structures.

TABLE 5 THE HIGHEST PCE% AND THE LOWEST PCE% IN THE DISTINCT STRUCTURE RESPECTIVELY.

| PCE% range | Structures | Jsc(mA /cm²) | Voc (V) | FF | PCE% |
|---|---|---|---|---|---|
| The Highest | FTO/ITO/ $RbGeBr_3$ / PEDOT: PSS / Au | 14.472 | 0.96 | 0.82 | 11.37 |
| The Lowest | FTO/TiO2/ $RbGeBr_3$ /Cu SCN/Au | 14.467 | 0.90 | 0.81 | 10.58 |

## V. CONCLUSION

In this research, two various PSCs were studied, with a focus on investigating the potential of $RbGeBr_3$ as a light-absorbing mineral perovskite active layer. Among the desired architectures, the highest PCE 11.373%, with a short-circuit current of 14.472 mA/cm$^2$ and an open-circuit voltage of 0.96

V related to FTO/ITO/$RbGeBr_3$/PEDOT: PSS/Au which was the first structure. Furthermore, the PCE of another structure is 10.580%, refer to the second structure. Furthermore, the maximum PCE was calculated in both structures at thicknesses of 80 nm for the ETL, 200 nm for the light-absorbing mineral layer, and 300 nm (constant value) for the HTL. Additionally, in this study, the effect of temperature increases on both structures was calculated in the conditions that had the highest efficiency. The overall results indicate that the second structure, FTO/$TiO_2$/$RbGeBr_3$/CuSCN/Au, is more stable at temperature. The PCE at 300 K is 10.58% reaching 6.17% at 450 K, which shows a 4.43unit difference. These results confirm the idea that a variety of factors have a significant impact on PSCs efficiency. The choice of semiconductor material utilized for various layers, the optimal thickness of these layers, and the environmental temperature are some of the important key factors that play a more prominent role in determining the overall efficiency of the solar cell. The objective of this article was to examine how a solar cell's light-absorbing material behaves when its light input power is 100 $mW/cm^2$, and it also calculates acceptable outcomes. As a consequence, these structures can be enhanced in the upcoming research, and the outcomes can be computed using a light input power of 1000 $W/m^2$.This research report could serve as a useful reference for future investigations of this material in more intricate cells to enhance PCE.

## VI. References


[1] T.C. Sum and N. Mathews, "Advancements in perovskite solar cells: photophysics behind the photovoltaics. Energy & Environmental Science", 7(8), pp.2518-2534, 2014.

[2] J.H. Lee, I.S., Jin and J.W. Jung, "Binary-mixed organic electron transport layes for planar heterojunction perovskite solar cells with high efficiency and thermal reliability". Chemical Engineering Journal, 420, p.129678, 2021.

[3] Z. Li, Y. Gao, Z. Zhang, Q. Xiong, L. Deng, X. Li, Q. Zhou, Y. Fang, and P. Gao, "cPCN-Regulated SnO 2 composites enables perovskite solar cell with efficiency beyond 23%. Nano-micro letters", 13, pp.1-16, 2021.

[4] S.M. Lawal, N. Fough, N. Sellami and f. Muhammad-Sukki, "Modeling and Simulation of Heterojunction Solar Cell; Determination of Optimal Values", 21st IEEE Interregional NEWCAS Conference (NEWCAS) (pp. 1-2). IEEE, 2023.

[5] H. Wang, Z. Dong, H. Liu ,W. Li ,L. Zhu ,H. Chen, "Roles of organic molecules in inorganic CsPbX3 perovskite solar cells". Advanced Energy Materials. 2021 Jan;11(1):2002940

[6] S. Sahare, H.D. Pham, D. Angmo, P. Ghoderao, J. MacLeod, S.B. Khan, S.L. Lee, S.P. Singh, and P. Sonar, "Emerging perovskite solar cell technology: remedial actions for the foremost challenges". Advanced Energy Materials, 11(42), 2021, p.2101085

[7] M.A. Green, A. Ho-Baillie, and H.J. Snaith, "The emergence of perovskite solar cells", Nature photonics, 8(7), 2014, pp.506-514

[8] M.K. Hossain, G.I. Toki, J. Madan, R. Pandey, H. Bencherif, H., M.K. Mohammed, M.R. Islam, MH.K. Rubel, M.F. Rahman, S. Bhattarai, and D.P. Samajdar, "A comprehensive study of the optimization and comparison of cesium halide perovskite solar cells using ZnO and Cu 2 FeSnS 4 as charge transport layers", New Journal of Chemistry, 2023, 47(18), pp.8602-8624

[9] L.J. Chen, C.R. Lee, Y.J. Chuang, Z.H. Wu, and C. Chen, "Synthesis and optical properties of lead-free cesium tin halide perovskite quantum rods with high-performance solar cell application". The journal of physical chemistry letters, 7(24), 2016, pp.5028-5035.

[10] A. Tooghi, A., D. Fathi, and M. Eskandari, "Numerical study of a highly efficient light trapping nanostructure of perovskite solar cell on a textured silicon substrate", Scientific Reports, 10(1), 2020, p.18699

[11] M. Kulbak, S. Gupta, N. Kedem, I. Levine, T. Bendikov, G. Hodes, and D. Cahen, "Cesium Enhances Long-Term Stability of Lead Bromide Perovskite-Based Solar Cells" , journal of physical chemistry letters, 7(1), pp.167-172, Jan. 2016.

[12] R. Wang, M. Mujahid, Y. Duan, Z.K. Wang, J. Xue, and Y. Yang., "A review of perovskites solar cell stability," Wiley Online Libr., vol. 29, no. 47, Nov. 2019, doi: 10.1002/adfm.201808843.

[13] V. D'innocenzo, G. Grancini, M.J. Alcocer, A.R.S. Kandada, S.D. Stranks, M.M. Lee, G. Lanzani, H.J. Snaith, and A. Petrozza, "Excitons versus free charges in organo-lead tri-halide perovskites", Nature communications, 5(1), 2014, p.3586.

[14] J.S. Manser, P.V. Kamat, "Band filling with free charge carriers in organometal halide perovskites", Nature Photonics. 2014 Sep;8(9):737-43

[15] S. Valizadeh, A. Shokri, A. Sabouri-Dodaran, N. Fough and F. Muhammad-Sukki, "Investigation of efficiency and temperature dependence in RbGeBr3-based perovskite solar cell structures", Results in Physics, 2024, 57, p.107351

[16] M. Houari, B. Bouadjemi, S. Haid, M. Matougui, T. Lantri, Z. Aziz, S. Bentata, and B. Bouhafs, "Semiconductor behavior of halide perovskites AGeX 3 (A= K, Rb and Cs; X= F, Cl and Br): first-principles calculations". Indian Journal of Physics, 2020, 94, pp.455-467

[17] Z.L. Yu, Q.R. Ma, B. Liu, Y.Q. Zhao, L.Z. Wang, H. Zhou, and M.Q. Cai, "Oriented tuning the photovoltaic properties of γ-RbGeX3 by strain-induced electron effective mass mutation", Journal of Physics D: Applied Physics, 50(46), 2017, p.465101

[18] F. Azri, A. Meftah, N. Sengouga and A. Meftah, "Electron and hole transport layers optimization by numerical simulation of a perovskite solar cell", Solar energy, 181, 2019, pp.372-378

[19] R. Pandey, and R. Chaujar, "Numerical simulations: Toward the design of 27.6% efficient four-terminal semi-transparent perovskite/SiC passivated rear contact silicon tandem solar cell", Superlattices and Microstructures, 100, 2016, pp.656-666

[20] T. Minemoto, M. Murata, "Impact of work function of back contact of perovskite solar cells without hole transport material analyzed by device simulation", Current Applied Physics, 14(11), 2014, pp.1428-1433

[21] T. Minemoto and M. Murata, "Device modeling of perovskite solar cells based on structural similarity with thin film inorganic semiconductor solar cells", Journal of applied physics, 2014, 116(5)

[22] L. Kavan, M. Grätzel, "Highly efficient semiconducting TiO2 photoelectrodes prepared by aerosol pyrolysis", Electrochimica Acta, 40(5), 1995, pp.643-652

[23] J.E. Jaffe, T.C. Kaspar, T.C. Droubay, T. Varga, M.E. Bowden and G.J. Exarhos, "Electronic and defect structures of CuSCN". The Journal of Physical Chemistry C, 114(19), 2010, pp.9111-9117

[24] Q. Zhang, C. S. Dandeneaunn, X. Zhou, and G. Cao, "ZnO nanostructures for dye-sensitized solar cells," Advanced Materials, vol. 21, no. 41, pp. 4087-4108, 2009.

[25] [25] S. Gavrilov, A. Dronov, V. Shevyakov, A. Belov, and E. Poltoratskii, "Ways to increase the efficiency of solar cells with extremely thin absorption layers", Nanotechnologies in Russia, vol. 4, no. 3, pp. 237-243, 2009.

[26] COMSOL Multiphysics User's Guide. 2012. p. 1–1292.

[27] S.A. Kalogirou, Solar Energy Engineering: Processes and Systems. 3rd ed. London, United Kingdom: Academic Press; 2023.

[28] I. Hamideddine, H. Zitouni, N. Tahiri, O. El Bounagui and H. Ez-Zahraouy, "A DFT study of the electronic structure, optical, and thermoelectric properties of halide perovskite KGeI 3-x Br x materials: photovoltaic applications", Applied Physics A, 127, 2021, pp.1-7

[29] G. Siefer and A.W. Bett, "Analysis of temperature coefficients for III–V multi-junction concentrator cells", Progress in Photovoltaics: Research and Applications, 22(5),2014, pp.515-524